Physica Medica 60 (2019) 150–155

Contents lists available at ScienceDirect

Physica Medica

journal homepage: www.elsevier.com/locate/ejmp

Original paper

Evaluation of the MOSkin dosimeter for diagnostic X-ray CT beams

L. Mendes Pereira[b,*], H.J. Khoury[a], M.E.A. Andrade[a], V.S.M. Barros[a], D. Cutajar[c], A.B. Rosenfeld[c]

[a] Federal University of Pernambuco, Recife, Brazil
[b] University Hospital of Würzburg, Würzburg, Germany
[c] Wollongong University, Wollongong, Australia

ARTICLE INFO

Keywords:
MOSkin
MOSFET
CT dosimetry

ABSTRACT

The aim of the present study was to evaluate the response of the MO*Skin* MOSFET dosimeter for X-ray diagnostic CT beams. Experiments were performed to investigate the sensitivity, energy dependence, reproducibility, fading and angular dependence of the dose response for the device. The dosimeter's performance was evaluated for the standard radiation qualities RQT 8, RQT 9 and RQT 10 in a metrology laboratory. In a CT scanner, the MO*Skin* was used to assess the air kerma profile and the dose profile in a phantom. The integral of the dose profile was compared to the $C_{PMMA,100}$ measured with a pencil ionization chamber. The results showed that the MO*Skin* response was linear and reproducible with doses in the CT range. Energy dependence varied up to a factor of 1.19 among the tested X-ray energies. Angular dependence of the response was not greater than 7.8% within the angle range from 0 to 90 degrees. Signal fading within 3 min was negligible. Additionally, the MO*Skin* was able to accurately assess the air kerma profile and the integral of the dose profile in a CT scanner. The integral of the dose profile in a phantom was in agreement with the $C_{PMMA,100}$. The presented results demonstrated the potential of the MO*Skin* for application in CT dosimetry.

1. Introduction

In recent years, solid-state radiation detectors, based on the metal oxide-silicon semiconductor field effect transistor (MOSFET), have gained widespread use as *in-vivo* dosimeters, especially for high-energy photon beams [1–4].

One designed version, called MO*Skin*, was developed based on real-time MOSFET technology by the Centre for Medical Radiation Physics (CMRP) at the University of Wollongong [5–7]. MO*Skin* dosimeters are able to natively measure skin dose at a depth of 0.07 mm and they were already validated for photon beam dosimetry in radiation therapy [6,8–10]. Nevertheless, the performance of the MO*Skin* in Computed Tomography (CT) has not been investigated. Thus, this research aimed to characterize the MO*Skin* dosimeter for X-ray CT beams within a quality control program.

Initially, the dosimeter's response was evaluated in a metrology laboratory for the standard radiation qualities RQT 8, RQT 9 and RQT 10, defined by the International Electrotechnical Comission (IEC) [11]. The sensitivity, energy dependence, reproducibility, angular dependence and fading of the dose-response for the device were investigated.

Additionally, measurements in a clinical setup were performed. The air kerma profile in a CT scanner was evaluated using an array of MO*Skin* dosimeters and the results were compared to TDL-100 dosimeters and a Gafchromic XR CT film. The MO*Skin* was also used to assess the integral of the dose profile in a phantom and its performance was compared to a pencil type ionization chamber.

2. Materials and methods

The MO*Skin* detector consists of a semiconductor MOSFET, measuring 0.8 mm × 0.6 mm × 0.35 mm in size, with a 0.55 μm thick gate oxide layer. The MOSkin is located at the tip of Kapton (polyamide) probe, as seen in Fig. 1. The probe differs from other commercially available MOSFET dosimeters, as it is built flat, without an epoxy layer covering the sensor. In this case, the buildup layer was designed to reproduce a water equivalent depth of 0.07 mm. The MO*Skin's* response is monitored by a battery-operated electrometer, dubbed Computerized Semiconductor Dosimetric System (CSDS).

The basic principle of using a MOSFET dosimeter involves monitoring the threshold voltage (Vth), which is altered when the device is exposed to ionizing radiation. The threshold voltage change is proportional to the number of trapped holes in the gate oxide, and therefore proportional to the dose deposited in the gate oxide layer. Thus, the delivered dose is equivalent to:

$$\Delta Vth = Vth - Vth_o \quad (1)$$

* Corresponding author at: Department of Diagnostic and Interventional Radiology, University of Würzburg, Oberdürrbacher Str. 6, D-97080 Würzburg, Germany.
E-mail address: e_pereira_L@ukw.de (L. Mendes Pereira).

https://doi.org/10.1016/j.ejmp.2019.03.030
Received 4 December 2018; Received in revised form 13 March 2019; Accepted 28 March 2019
Available online 05 April 2019

Fig. 1. MO*Skin* probe.

where Vth_o is the initial threshold voltage reading (before the irradiation) and Vth is the post-irradiation threshold voltage reading.

The change in threshold voltage was measured with the CSDS, which allows up to 5 MO*Skin*s to be read simultaneously and has an accuracy of ±1 mV. Further structural and operational details of the MO*Skin* may be found in Ref. [5].

2.1. Evaluation in standard radiation field

The performance characteristic of the MO*Skin* was evaluated at the Metrology Laboratory of Ionizing Radiation from the Federal University of Pernambuco (also known as LMRI), using the standard radiation fields RQT 8, RQT 9 and RQT 10. These standard qualities are defined by IEC and their metrological terms, definitions and methods are described in Ref. [11].

The RQT radiation beams were calibrated in the presence of a high-frequency X-ray equipment, operating in the voltage range from 10 to 320 kV. The standard dosimetric system for this setup is a PTW Freiburg TW 30,009 ionization chamber, certified by the Physikalisch-Technische Bundesanstalt (PTB), connected to a PTW Unidos 10,001 electrometer. Environmental conditions were kept constant and the consistency of the X-ray beam intensity was verified by a monitor ionizing chamber coupled to the X-ray tube during measurements. Table 1 presents the air kerma rates and reference parameters of the X-ray qualities used. Experimental uncertainties were smaller than 2.5% (confidence level of 95%).

Fig. 2 shows the experimental setup used to evaluate the MO*Skin*'s response in a free-in-air geometry. The dosimeter was placed in the beam's central axis, facing the X-ray tube.

2.1.1. Reproducibility

To investigate the individual detector reproducibility, three randomly selected MO*Skins* were irradiated and their response was evaluated for the beam quality RQT 9. As the MO*Skin* readout unit provides a measurement of the threshold voltage to the nearest mV, taking into account both the pre-irradiation reading and the post-irradiation reading, the change in threshold voltage will have an uncertainty of 1 mV (in the readout alone). For each reading, the MO*Skin* was irradiated three times at air kerma value of 52.3 mGy, in order to obtain an accumulated response above 100 mV and reduce the impact of the electrometer's display accuracy to less than 1%. The MO*Skin*'s response in mV was then divided by the number of irradiations. This procedure was consecutively repeated ten times, and a coefficient of variation was calculated for each dosimeter from these ten different measurements.

Table 1
RQT radiation qualities used to evaluate the MO*Skin*'s performance.

Quality of the beam	X-ray tube voltage (kV)	Effective Energy (keV)	1st HVL (mm Al)	Air kerma rate (mGy/min)
LMRI-RQT 8	100	48.0	6.89	13.20
LMRI-RQT 9	120	55.6	8.50	17.42
LMRI-RQT 10	150	65.1	10.26	30.16

2.1.2. Short term fading

Even though MOSFET detectors store the dose information for a long time, trapped charges can gradually fade after irradiation. In the present study, a post-exposure response test was performed with a MO*Skin* dosimeter irradiated with 87.1 mGy (RQT 9). Consecutive readings of ΔVth were obtained for 10 min and the signal fading effect was evaluated. The first reading was performed 10 s after the irradiation. All the consecutive readings were taken at regular intervals of 30 s.

2.1.3. Air kerma response and energy dependence

The air kerma response was assessed for each RQT beam quality and the MO*Skin*'s sensitivity was investigated by plotting the threshold voltage change as a function of the delivered air kerma. For comparability across the different range of kilovoltages, the energy dependence of the device was calculated using the MO*Skin*'s sensitivity for the RQT 9 X-ray quality as a reference.

2.1.4. Angular dependence

The angular dependence of the sensor's response was performed free-in-air in a housing constructed support. For this purpose, the MOSFET dosimeter was rotated around the z-axis (as seen in Fig. 3) and irradiated with incident X-ray beams at angles from 0 to 90 degrees.

The angular dependence of the MO*Skin* dosimeter was evaluated for the RQT 9 reference beam. Using the same air kerma, ΔVth measurements were performed for each angle and the results were normalized to the 0 degrees reading for the correspondent axis of rotation.

2.2. Study in clinical field

2.2.1. Air kerma profile assessment

An array of five MO*Skin* dosimeters, previously characterized for the radiation beam RQT 9, was used to study the air kerma profile in a clinical Philips CT scanner, model Brilliance 6. The dosimeters were arranged side-by-side and fixed on the top of a Styrofoam surface, as shown in Fig. 4(A). The arrangement was placed on the scanner's table and translated across the X-ray beam in steps of 6 mm. In each step, five expositions in the axial mode were made, with a collimation (NT) of 24 mm, 120 kV and 250 mAs. The output of each MO*Skin* was divided by the number of exposures and converted to mGy using their respective sensitivity coefficients.

The array was approximately 15 mm long, thus overlapping of measurement points occurred when the table was translated. In this case, the mean air kerma for that position was calculated.

The results obtained with the MO*Skin* were compared to thermoluminescent dosimeters TLD-100 and Radiochromic film Gafchromic XR CT.

A setup with 50 TLDs-100 positioned side by side, as shown in Fig. 5, was used. The length of the TLD setup was 200 mm. The array remained fixed at the center of the beam (Fig. 5), and three exposures were performed using the previously described irradiation parameters. The TLD response was measured using a Victoreen 2800 M reader and integration of the glow curve area was in the region of 110 °C to 300 °C.

Measurements of the CT radiation profile were also performed using a 150 mm Gafchromic XR CT film. The film was positioned in the center of the X-ray beam and three exposures were executed. After, the optical density of the film was measured using an X-rite reflection densitometer, model 530. The measurements were performed along the entire longitudinal axis of the film, in steps of 5 mm.

The air kerma profile measured with each dosimeter was then compared by plotting their normalized responses as a function of their location along the central axis of the radiation beam.

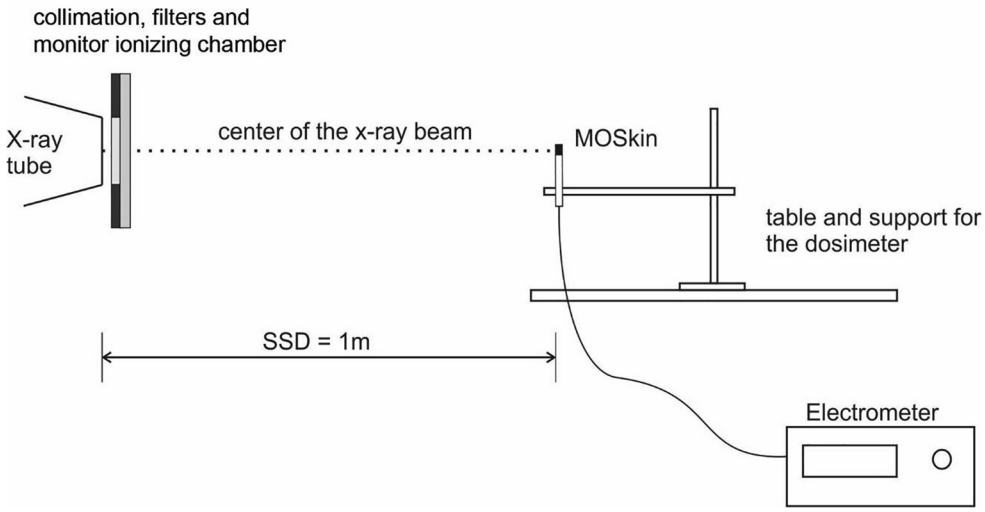

Fig. 2. Experimental Setup used to evaluate the MO*Skin* response in the calibration laboratory.

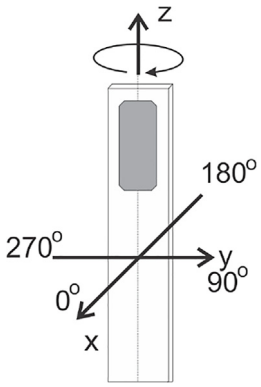

Fig. 3. Angular dependence irradiation geometry.

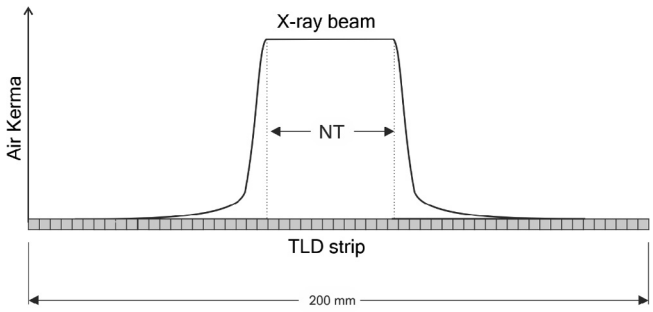

Fig. 5. Setup of TLDs to measure the air kerma profile in TC. Fifty TDLs were used.

2.2.2. Accumulated dose assessment

With the increase of beam widths and the advent of multiple-slice and helical scanners, concerns related to the current dose measurement protocols and instrumentation in computed tomography (CT) have arisen [12,13]. The current methodology of dose evaluation, which is based on the measurement of the integral of a single slice dose profile using a 100 mm long cylinder ionization chamber ($C_{a,100}$ and $C_{PMMA,100}$), has been shown to be inadequate for wide beams, as it does not collect enough of the scatter-tails radiation to make an accurate measurement [12,13]. An alternative approach has been proposed in the AAPM Report number 111 [14]. In this new protocol, the accumulated dose (D_L) is obtained by the integral of the dose profile, measured by translating small detectors through the beam plane. This method can be used for measurements of any arbitrary length in phantoms or in the air.

Thus, to evaluate the viability of the MO*Skin* detector to measure the accumulated dose, the dosimeter was fit inside a PMMA rod and placed in the central hole of a PMMA dosimetric head phantom (diameter of 16 cm), as visualized in Fig. 6A. Using the center of the radiation beam as reference, the dosimeter was translated along the axis of rotation of the X-ray tube, and readings were collected on this axis over ± 50 mm. For each measurement, five expositions were made,

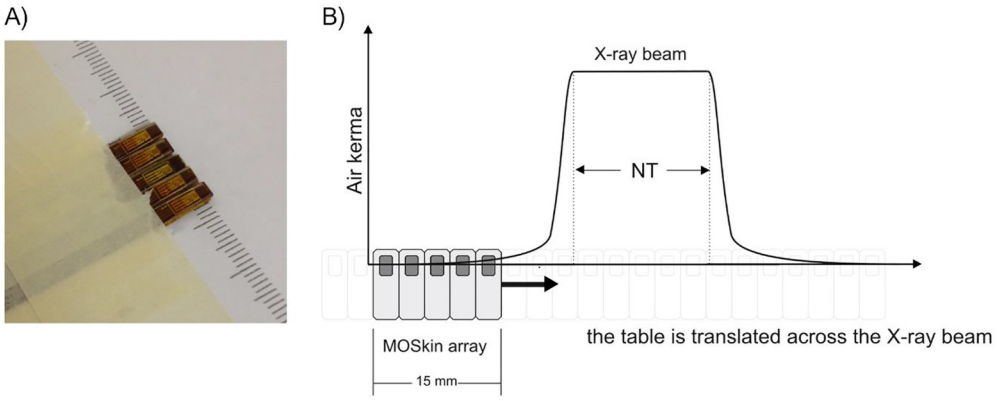

Fig. 4. Arrangement to obtain the air kerma profile in CT. The setup with five MO*Skin* detectors is seen in A) and an illustration of the measurement is presented in B).

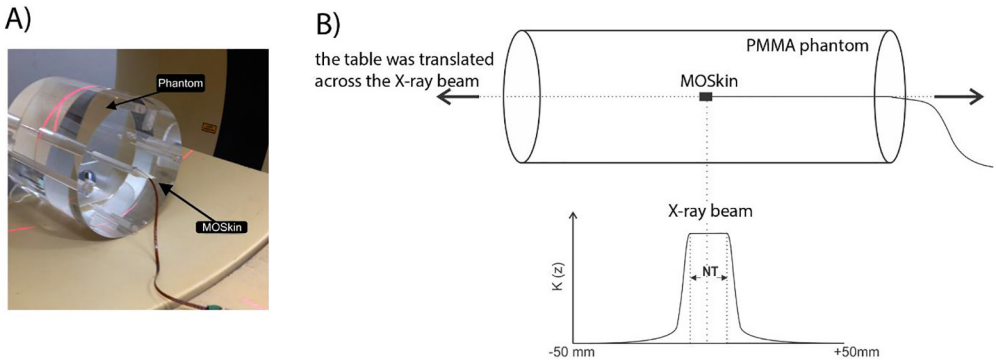

Fig. 6. Experimental setup to estimate the accumulated dose (D_L) calculated as the integral of the dose profile over a length (L) of 100 mm, which should be equivalent to the $C_{PMMA,100}$ accessed with a pencil ionization chamber.

with full axial rotation, collimation of 9 mm, 250 mAs and 120 kV. The accumulated dose was calculated as the integral of the dose profile over a length (L) of 100 mm.

Measurements were performed with the same setup using a pencil ionization chamber (PTW Freiburg TW 30009). The D_L measured with the MO*Skin* was then compared with the air kerma index in the center of the phantom ($C_{PMMA,100}$), assessed with the pencil ionization. For the $C_{PMMA,100}$ calculation, the center of the phantom was aligned with the center of the radiation beam and five exposures were made.

2.2.3. Reproducibility and dose uncertainty

To test the reproducibility of the MO*Skin*'s response in the CT scanner, three measurements were performed with a previously calibrated MO*Skin* for the RQT 9 beam quality. The MO*Skin* was placed in the central hole of the PMMA phantom, and the center of the phantom/MO*Skin* was aligned with the centermost point of the X-ray beam. For each measurement, five exposures in the axial mode were executed, with full axial rotation, collimation of 9 mm, 250 mAs and 120 kV. A coefficient of variation was then calculated from these measurements. For comparison, the experiment was also performed with the pencil ionization chamber.

The combined standard uncertainty associated with the dosimeter was calculated as in Ref. [15]. All sources of uncertainties were identified and classified as Type A or Type B as per ISO/IEC Guide 98-1:2009 classification [16]. The following sources of uncertainties were considered: calibrations uncertainties in standard field, MO*Skin*'s reproducibility in the clinical field, readout equipment uncertainties, fading of the response and the maximum angular dependence. Energy dependence was not considered, because the MOSFET was calibrated specifically for the RQT 9 beam quality, with 120 kV.

3. Results

3.1. Evaluation in the standard radiation field

A linear dose response was observed for the RQT 8, RQT 9 and RQT 10 X-ray standard beam qualities, as seen in Fig. 7 (in most of the cases, the standard deviation error bars were smaller than the markers and cannot be visualized).

The gradient of each plot gives the MO*Skin* sensitivity for a single MO*Skin* as follows: 0.921 mV/mGy, 0.769 mV/mGy and 0.672 mV/mGy, for the RQT 8, RQT 9 and RQT 10 X-ray beams respectively. Similar results were found in reference [8], where the MO*Skin* response was studied for kilovoltages X-ray energies.

Assuming the sensitivity of 0.672 mV/mGy, the minimum detectable dose was 1.49 mGy (1 mV of threshold voltage increase). However, this will be associated with the readout uncertainty of ± 1 mV, which in this case is equivalent to a dose uncertainty of ± 1.49 mGy. For larger doses, the readout uncertainty is still ± 1.49 mGy, but the fractional/percentage error is reduced.

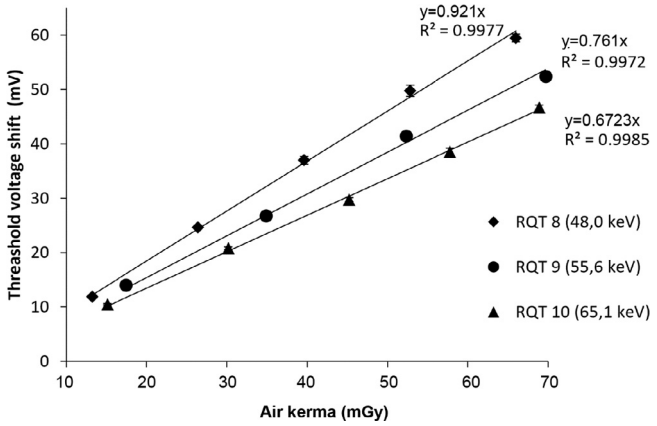

Fig. 7. MO*Skin's* linearity for RQT X-ray beam qualities. The MO*Skin* response was linear for all tested energies, with a maximum response for the RQT 8 beam. Most of the error bars are smaller than the markers and are not visible.

As the beam quality decreases, the MO*Skin* energy response increases, with a maximum energy response for RQT 8. This is due to the photoelectric effect, which is the dominant energy transfer mechanism at lower photon energies in the silicon dioxide layer. The energy dependence varied up to a factor of 1.19 among the tested X-ray energies (response normalized for RQT 9).

3.2. Individual reproducibility

The randomly selected MO*Skin* detectors presented different mean sensitivities for the irradiated air kerma (52.3 mGy/RQT 9), ranging from 0.587 to 0.759 mV/mGy. The coefficient of variation (COV) of their responses varied between 1.33% and 6.15%, showing good agreement with the literature [17,18]. The results from this experiment are presented in Table 2.

3.3. Short-term fading

The MO*Skin*'s first measurement, 10 s after the irradiation, corresponded to an initial ΔVth equal to 74 mV for RQT 9 and an air kerma of 87.1 mGy. During the first 3 min, ΔVth oscillated within the reader accuracy of ± 1 mV, i.e. no measurable fading was observed for multiple readouts. After 10 min, ΔVth had decayed by 9.5% of its initial value.

3.4. Angular dependence

The angular dependence of MO*Skin* dosimeter, evaluated for the

Table 2
Results of the reproducibility test. For each reading, the MO*Skin*s were irradiated three times, with an air kerma of 52.3 mGy. The values presented in the table were divided by the number of irradiations.

MO*Skin*	MO*Skin* reading (mV)										Mean reading (mV)	CV (%)	Mean sensitivity (mV/mGy)
1	40	38	41	39	41	40	40	38	41	39	39.7	2.92	0.759
2	40	40	40	40	41	40	40	40	41	40	40.0	1.33	0.766
3	33	32	31	28	32	31	33	28	30	29	30.7	6.15	0.587

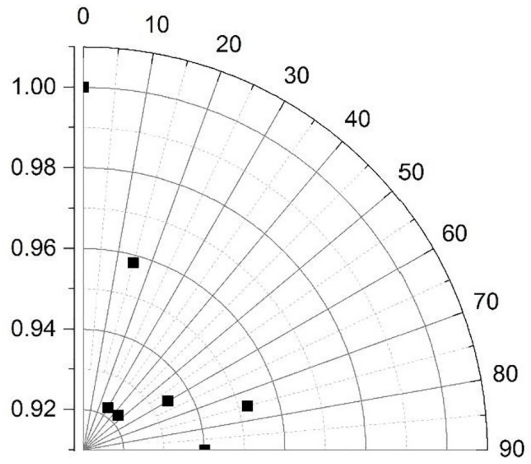

Fig. 8. Angular Dependence of the MO*Skin* in free-in-air geometry was reduced only by 6% when irradiated at an angle of 90 degrees. At 30 and 45 degrees, the response was reduced by almost 8%.

RQT 9 computed tomography reference beam, is shown in Fig. 8.

The angular response for the MO*Skin*, placed free in the air, was not greater than 7.8%, within an angle range from 0 to 90 degrees. At 90 degrees, its response was only 6% smaller than at 0 degrees.

3.5. Evaluation in the clinical field

Fig. 9 shows the air kerma profile measured with the MO*Skin* setup, the Gafchromic film and the TLD-100.

It is possible to observe that the three dosimeters were able to depict the beam profile, but the MOSkin and the TDL 100 presented oscillation in the plateau, especially when compared to the Gafchromic XR CT film, which is the standard choice for this application. As presented by Ref. [19], the oscillation of the Gafchromic film was within the dosimeter uncertainty (± 5%).

The dose profile measured with the MO*Skin* in the center of the PMMA phantom is presented in Fig. 10.

The Accumulated Dose, calculated as the integral of the dose profile, was 39.7 ± 0.99 mGy. The $C_{PMMA,100}$ value obtained with the ionization chamber was 37.9 ± 0.15 mGy. Student's *t*-test have shown that both values are statistically identical, within a 95% confidence interval.

The coefficient of variation of the response of the MO*Skin* was 2.47% in the CT scanner. The ionization chamber presented a CV of only 0.4%.

Other components of the experimental uncertainties were: 2.5% due to calibration curve of the MO*Skin*, 0.8% from the electrometer readout, 1% due to fading of the response under three minutes and 7.8% due to the maximum angular response. The combined standard uncertainty was then 4.83%, with an expanded uncertainty (k = 2) of 9.66%.

4. Discussion and conclusion

In this study, the MO*Skin* was evaluated for standard CT X-ray beams in a metrology laboratory and in a CT scanner. It has been shown that its response is reproducible and sensitive enough to measure doses at the diagnostic X-ray levels.

As expected from a semiconductor, MO*Skin* exhibited a significant energy response, particularly at low photon energies. The energy dependence was consistent among different dosimeters, which indicates that the MO*Skin* could be calibrated for a single X-ray beam quality and its sensibility factor could be calculated for the others.

The angular dependence, when irradiated in the air, was not greater than 7.8% within the angle range from 0 to 90 degrees. As the angular dependence of the MOSkin is mainly due to geometrical influences of the packaging, the response of the MOSkin with angle of incidence is sinusoidal. By placing two detectors in a face to face arrangement and averaging the readings, the angular dependence can be greatly reduced [20].

In the scanner, the semiconductor dosimeter was able to accurately measure the air kerma profile of the X-ray beam and the dose profile in the center of the PMMA phantom. The accumulated dose, measured in the phantom over a length of 100 mm, was found to be statistically similar to the $C_{PMMA,100}$ measured with a pencil ionization chamber.

Therefore, it's possible to conclude that the MO*Skin* presents itself as a promising alternative for dose evaluation in CT. Nevertheless, its performance has not yet been compared against the standard IEC 61674:2012 [21].

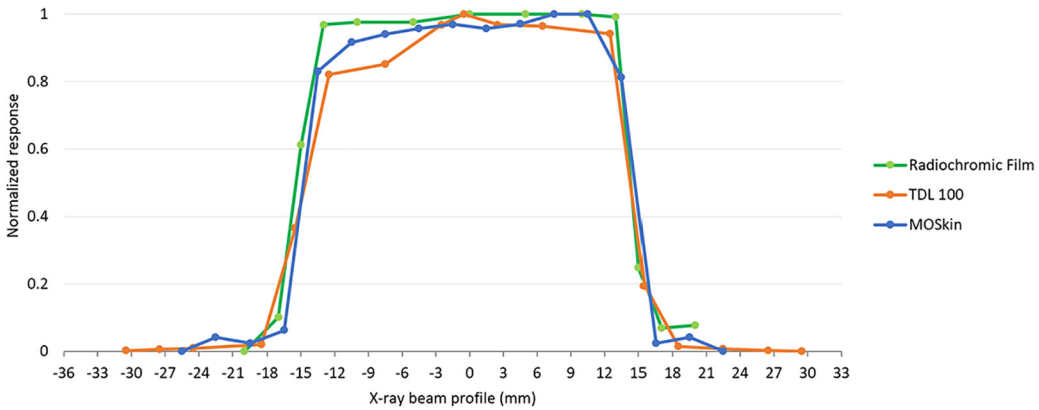

Fig. 9. Air kerma profile obtained with the MO*Skin*, Radiochromic film and TLDs. For comparison, the response of the dosimeters was normalized to one.

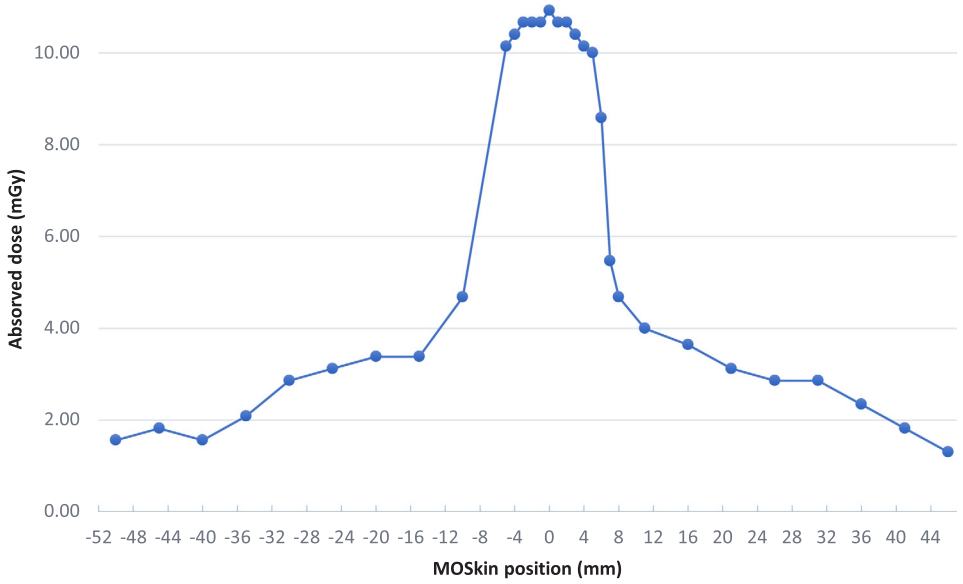

Fig. 10. The dose profile measured with a MO*Skin* dosimeter represents the dose distribution in the PMMA head phantom with good accuracy.

Acknowledgements

This work was supported by FACEPE, Brazil (APQ 0648-3.09/14). One of the authors, (Mendes Pereira, L.) is grateful to CAPES and CNPq for the provided fellowships.

References

[1] Alnawaf H, Butson M, Yu PKN. Measurement and effects of MOSKIN detectors on skin dose during high energy radiotherapy treatment. Australas Phys Eng Sci Med Sep. 2012;35(3):321–8.
[2] Kumar AS, Sharma SD, Ravindran BP. Characteristics of mobile MOSFET dosimetry system for megavoltage photon beams. J Med Phys 2014;39(3):142–9.
[3] Kron T, Rosenfeld A, Lerch M, Bazley S. Measurements in radiotherapy beams using on-line MOSFET detectors. Radiat Prot Dosim 2002;101(1–4):445–8.
[4] Al-Mohammed HI. Evaluation of clinical use of OneDose metal oxide semiconductor field-effect transistor detectors compared to thermoluminescent dosimeters to measure skin dose for adult patients with acute lymphoblastic leukemia. N Am J Med Sci 2011;3(8):362–6.
[5] Alshaikh S, Carolan M, Petasecca M, Lerch M, Metcalfe P, Rosenfeld A. Direct and pulsed current annealing of p-MOSFET based dosimeter: the 'MOSkin'. Australas Phys Eng Sci Med 2014;37(2):311–9.
[6] Alshaikh SM. Mosfet annealing and interface dosimetry in complex radiation therapy. University of Wollongong; 2012.
[7] A. Rozenfeld, Radiation sensor and dosimeter (MOSkin), PCT/AU2008/000788; 03-Jun-2014.
[8] Lian CPL. Characterisation and application of the MOSkin radiation dosimeter at clinical kilovoltage X-ray energies. University of Wollongong; 2013.
[9] Gambarini G, et al. Online in vivo dosimetry in high dose rate prostate brachytherapy with MOSkin detectors: in phantom feasibility study. Appl Radiat Isot Jan. 2014;83(Pt C):222–6.
[10] Qi Z-Y, et al. In vivo verification of superficial dose for head and neck treatments using intensity-modulated techniques. Med Phys 2009;36(1):59.
[11] IEC, IEC 61267 : Medical diagnostic X-ray equipment – Radiation Conditions for use in the determination of characteristics. Geneva: IEC; 2005.
[12] Dixon RL. Restructuring CT dosimetry-A realistic strategy for the future Requiem for the pencil chamber. Med Phys 2006;33(10):3973.
[13] Dixon RL, Ballard AC. Experimental validation of a versatile system of CT dosimetry using a conventional ion chamber: Beyond CTDI[sub 100]. Med Phys 2007;34(8):3399.
[14] AAPM. Comprehensive Methodology for the Evaluation of Radiation Dose in X-Ray Computed Tomography: AAPM report 111. College Park; 2010.
[15] IAEA, Measurement Uncertainty: A Practical Guide for Secondary Standards Dosimetry Laboratories, no. 1585. Vienna: International Atomic Energy Agency; 2008.
[16] ISO, ISO GUIDE 98-1:2009(E) Uncertainty of measurement — Part 1 : Introduction to the expression of uncertainty in measurement; 2010.
[17] Lian CPL, et al. Measurement of multi-slice computed tomography dose profile with the Dose Magnifying Glass and the MOSkin radiation dosimeter. Radiat Meas 2013;55:51–5.
[18] Brady SL, Kaufman Ra. Establishing a standard calibration methodology for MOSFET detectors in computed tomography dosimetry. Med Phys 2012;39(6):3031–40.
[19] Tomic N, et al. Characterization of calibration curves and energy dependence GafChromic™ XR-QA2 model based radiochromic film dosimetry system. Med Phys 2014;41(6Part1):062105.
[20] Hardcastle N, et al. In vivo real-time rectal wall dosimetry for prostate radiotherapy. Phys Med Biol Jul. 2010;55(13):3859–71.
[21] IEC, IEC 61674: Medical electrical equipment - Dosimeters with ionization chambers and/or semiconductor detectors as used in X-ray diagnostic imaging; 2012.